Published in final edited form as:
Appl Radiat Isot. 2008 September ; 66(9): 1175–1182. doi:10.1016/j.apradiso.2008.01.012.

Imaging and Dosimetry of ^{99m}Tc EC Annexin V: Preliminary Clinical Study Targeting Apoptosis in Breast Tumors

Hiroaki Kurihara[1], **David J. Yang**[1,*], **Massimo Cristofanilli**[2], **William D. Erwin**[1], **Dong-Fang Yu**[1], **Saady Kohanim**[1], **Richard Mendez**[1], and **E. Edmund Kim**[1]

1*Department of Experimental Diagnostic Imaging, The University of Texas M. D. Anderson Cancer Center, Houston, Texas 77030*

2*Department of Breast Medical Oncology, The University of Texas M. D. Anderson Cancer Center, Houston, Texas 77030*

Abstract

Background—Early detection of cellular events is important to predict the outcome of the patients. This study was aimed to use ^{99m}Tc EC-annexin V to image tumor cells undergoing apoptosis.

Methods—In ten patients with breast cancer, scintigraphic images and dosimetric estimates were obtained after administering ^{99m}Tc EC-annexin V.

Results—Nine of the 10 cases showed detectable ^{99m}Tc EC-annexin V uptake in tumor. Higher values of T/N ratios are associated with patient after treatment.

Conclusions—Apoptosiscan be quantified using ^{99m}Tc EC-annexin V.

INTRODUCTION

Breast cancer is the second leading cause of death among women with cancer. The use of adjuvant systemic therapies has contributed to improve the prognosis in women with primary breast cancer (PBC) (1). In the last decade there has been a more widespread use of induction chemotherapy (IC) and radiation therapy (RT) in the management of women with primary disease. The advantage of this approach is primarily related to the possibility of down-staging the disease to allow for a more conservative surgical approach. Additionally, the evaluation of tumor response after completion of IC and/or RT, particularly the amount of pathological residual disease, provides us prognostic information (2). The National Surgical Adjuvant Breast and Bowel Project (NSABP) completed a randomized trial (B-18) to evaluate if IC resulted in a better outcome than postoperative chemotherapy (both groups received doxorubicin and cyclophosphamide) (3). The study of 1,523 randomized patients did not demonstrate a statistical significant difference in disease-free survival (DFS) nor overall survival (OS) between the two groups. A significant advantage in DFS was found only in patients achieving a pathological complete response (pCR) compared to the other groups achieving a pathological partial response (pPR) or no response. In the last decade, the extensive use of taxanes in regimens as IC has improved the achievement of pCR. However, the effects

*Address correspondence to: David J. Yang, Ph.D., The University of Texas M. D. Anderson Cancer Center, Experimental Diagnostic Imaging, Box 59, 1515 Holcombe Boulevard, Houston, Texas 77030, Tel: (713) 794-1053, Fax: (713) 794-5456, E-mail: dyang@di.mdacc.tmc.edu.

on long-term prognosis have still to be determined (4,5). We reported the preliminary analysis of a randomized neo-adjuvant protocol comparing a weekly schedule vs. an every three-week schedule of paclitaxel (5). The results showed a significant difference in pCR between the weekly schedule (pCR= 30.8%) compared to the every 3 weeks (pCR=11.4%).

With the increasing availability of effective, cytotoxic and biological agents, the possibility to have reliable and reproducible predictors of overall response could provide the opportunity to appropriately select patients for more targeted and efficacious treatments early in their treatment phase. The use of gene-array profiling has been indicated as one diagnostic modality able to identify more accurately patients with higher likelihood of complete pathological response (pCR) to IC (6). Another possible alternative approach to the problem is represented by the use of more advanced imaging modalities (functional imaging) that are able to describe the biological phenomenon associated with a specific treatment. The occurrence of treatment-related apoptosis in patients receiving cytotoxic treatments is an interesting and significant area of investigation.

To characterize tumors, radiolabeled ligands, radiolabeled antibodies, and signal transduction agents have opened a new era and have undergone extensive preclinical development and evaluation (7,8). The strategy of labeling biomolecules for molecular imaging has generated considerable interest, but focus must first be on the stability and efficient attachment of isotopes. Several ^{99m}Tc-labeling techniques have been reported, and they include N_4 (e.g. DOTA), N_3S (e.g. MAG-3), N_2S_2 (e.g. ECD), NS_3, S_4 (e.g. sulfur colloid), DTPA, and HYNIC (9-14). The HYNIC technique requires two additional chemicals (tricine, triphenylphosphine) in order to form a ^{99m}Tc complex, thus making it inconvenient to formulate in a kit form and costly. The nitrogen and sulfur combination has been shown to be a stable chelator for ^{99m}Tc. Bis-aminoethanethiol tetradentate ligands, also called diaminodithiol compounds, are known to form very stable Tc-complexes on the basis of efficient binding of the oxotechnetium group to two thiolsulfur and two amine nitrogen atoms. ^{99m}Tc-ethylenedicysteine (^{99m}Tc-EC) is a successful example of N_2S_2 chelates. Using a standard coupling technique, ^{99m}Tc-EC-drug conjugates were then developed to characterize tumor tissues (15,16). In the previous report, we have described in vivo biodistribution and planar imaging studies in tumor-bearing rats given ^{99m}Tc-EC annexin V (^{99m}Tc-EC-ANX), and have demonstrated the pharmacokinetic distribution of the tracer and feasibility of using ^{99m}Tc-EC-ANX to image apoptosis-induced tumor (17). In this report, we demonstrate the imagings of ^{99m}Tc EC-annexin V in women with PBC either before treatment (5 patients) or during the first cycle of IC (5 patients), and radiation dosimetry evaluation using image-based biodistribution analysis.

METHODS

Chemicals

N-hydroxysulfosuccinimide (Sulfo-NHS) and 1-ethyl-3-(3-dimethylaminopropyl) carbo-diimide-HCl (EDC) were purchased from Pierce Chemical Co (Radford, IL). All other chemicals were purchased from Aldrich Chemical Co (Milwaukee, WI). Silica gel coated thin-layer chromatography (TLC) plate was purchased from Whatman (Clifton, NJ). EC was prepared in a two-step synthesis according to the previously described methods (18,).

Mass spectral analyses were conducted at the University of Texas Health Science Center (Houston, TX). Nuclear magnetic resonance (NMR) spectra were recorded on a Bruker-300 Spectrometer. The mass data were obtained by fast atom bombardment on a Kratos MS 50 instrument (England).

Synthesis and Radiolabeling of EC-Annexin

EC-Annexin V was prepared according to the previously described methods (17). Briefly, Sodium bicarbonate (1N, 1 ml) was added to a stirred solution of EC (5 mg, 0.019 mmol). To this colorless solution, sulfo-NHS (4 mg, 0.019 mmol) and EDC (4 mg, 0.019 mmol) were added. Annexin V (M.W. 33 kD, human, Sigma Chemical Company) (0.3 mg) was then added. The mixture was stirred at room temperature for 24 hrs. The mixture was dialyzed for 48 hrs with cutoff at M.W.10,000. After dialysis, the product was freeze dried, with the product in the salt form weighing 0.5 mg. ^{99m}Tc-pertechnetate was obtained from Syncor Pharmaceutical Inc. (Houston, TX). Radiosynthesis of ^{99m}Tc-EC-annexin was achieved by adding the required amount of ^{99m}Tc-pertechnetate into EC-annexin (50 *mg*) and tin chloride (II) ($SnCl_2$, 100 *mg*). The mixture was loaded on a sephadex gel column (PD-10, G-25, Pharmacia Biotech, Swiss) and eluted with phosphate buffered saline (pH 7.4). One ml of each fraction was collected. The product was collected at fraction 3, yielding 70%. Radiochemical purity was assessed by Radio-TLC (Bioscan, Washington, DC) using 1M ammonium acetate: methanol (4:1) as an eluant. HPLC, equipped with NaI detector and UV detector (254 nm), was performed on a GPC column (Biosep SECS3000, 7.8 3 300 mm, Phenomenex, Torrance, CA) using a flow rate of 1.0 ml/min for 0.1% LiBr in PBS (10 mM, pH 5-7.4) as an eluant.

Clinical scintigraphic imaging studies

Patients—Clinical studies were conducted using ^{99m}Tc-EC-ANX in 10 breast cancer patients. The protocol was approved by the University of Texas M.D. Anderson Cancer Center Investigational Review Board (ID-02-732). Between December 2003 and February 2004, 10 patients with untreated primary breast cancer (stage II-III) were enrolled in this prospective study. Five of these patients received a dose of induction therapy 16 hours before the imaging session. The induction therapy consisted of chemotherapy (paclitaxel, 2 patients; fluorouracil, doxorubicin and cyclophosphamide (FAC), 1 patient) and bcl-2 antisense oligonucleotide therapy (Genasense™, 2 patients). The information of the patients or tumor biomarker such as age, stage/grade of the tumor, status of ER/PR, or erbB-2 were reviewed from the medical records.

Imaging—After a signed informed consent, they received a single intravenous injection of 925-1073MBq of ^{99m}Tc-EC annexin V. Subsequently, whole body planar images using a dual-headed gamma camera were obtained at 0.5, 2-4, 18-24 hour after injection. SPECT images of the chest were also obtained at 3hours post injection. Computer outlined regions of interest (ROI) (counts per pixel) were used to determine tumor-to-non tumor count density ratios (T/N ratio). Each ROI of the tumor was determined as a high accumulated area which matched to the tumor location in the breast. The opposite area in the other breast was determined as the ROI of the non-tumor tissue. The ratios were used to compare dynamic tumor uptake pre-and post-treatment. Errors in the use of image ROIs as standards to correspond to anatomically relevant features have been described and found tolerable.

Dosimetry—Based upon quantification of the serial whole body images (0.5, 2-4, 18-24 hours) from the clinical studies, percentage uptake of injection doses of whole body, blood-forming organ and gonad were calculated to generate estimated residence times of those organs, and then dosimetry of ^{99m}Tc EC-annexin V was estimated using MIRDose 3.1 (19).

RESULTS

Synthesis and Radiolabeling of EC-Annexin

A simple and efficient synthesis of ^{99m}Tc EC-annexin was developed (Figure 1). EC was conjugated to amino or lysine residue of annexin V. ^{99m}Tc EC-annexin was found to be radiochemically pure (100%). The retention time of ^{99m}Tc EC-annexin was at 9.63 min (Figure

2). Under the same conditions, the retention time of ^{99m}Tc-EC (control) was at 14.03 min (data not shown). The amount injected to HPLC was 111 kBq per 22.5 ng of ^{99m}Tc EC-annexin and the specific activity was calculated to be 185GBq/μmol.

Clinical scintigraphic imaging studies

Patients—The median age of the patients was 54 years (range 24-70). The median size of breast tumors was 4 cm (range 3-8 cm). The evaluation of standard biomarker demonstrated that 8 patients (80%) were estrogen receptor positive (ER+) and/or progesterone receptor positive (PR+). Additionally, a poorly differentiated Black's nuclear grade 3 was found in 6 patients. By means of fluorescence in situ hybridization (FISH), erbB-2 amplification was demonstrated in only 2 patients (20%). Clinical characteristics of these ten patients including tumor-to-non tumor count density ratios (T/N ratios), Ki-67 and the treatment response are summarized in Table 1. In one patient, the imaging data was not collected because of its unacceptable scintigraphic image due to colloidal formation during radiosynthesis.

Imaging—One of the ten patient showed high uptake in lung, indicating colloidal formation of ^{99m}Tc due to the use of an excess amount of tin chloiride (data not shown). In the remaining nine cases, there was detectable ^{99m}Tc EC-annexin V uptake that corresponded to the area of palpable invasive disease (Figure 3). Typical scintigraphic images of patients after treatment (case 4) and without treatment (case 9) were shown in Figure 4. The mean T/N ratio of 9 patients was 2.1 (range 1.3-3.3). There was a significant difference in the mean T/N ratios between those patients receiving IC and without IC (Figure 5). In those patients receiving IC, the mean T/N ratio was 2.6±0.5 (range 2.1-3.3, n=5), which was higher than those patients without IC (1.5±0.2, range 1.3-1.7, n=4). There was a trend such that a high T/N had a better response.

Dosimetry—Clinical-image based dosimetry revealed that the effective dose (ED) and effective dose equivalent (EDE) were calculated to be 6.30×10^{-3} mSv/MBq and 7.35×10^{-3} mSv/MBq, respectively. The total EDEs for the proposed single injection dosage of 925-1073 MBq of ^{99m}Tc EC-annexin V were evaluated to be 6.80-7.89 mSv. The liver showed a highest radiation absorbed dose of 9.35×10^{-6} Gy/MBq, and the radiation dose equivalent for the proposed single injection dosage to the liver were calculated to be 8.65-10.03 mSv (Table 2).

DISCUSSION

Screening mammography has been demonstrated to increase the early detection of invasive and pre-invasive breast cancer, even if it has a high false-negative rate in women with dense breast tissue and is not an accurate methodology for early accurate measurement of response or for prediction of therapeutic response (20). Similarly, ultrasonography and CT are not extremely accurate in predicting therapeutic response. MRI has been used to follow-up post-treatment changes, providing information about the perfusion and diffusion in tumors, with the status of blood flow (21). Improvement of scintigraphic tumor diagnosis, prognosis, planning, and monitoring of treatment of cancer will clearly be determined by the development of more tumor-specific radiopharmaceuticals. Radionuclide imaging modalities (positron emission tomography, PET; single photon emission computed tomography, SPECT) are diagnostic cross-sectional imaging techniques that map the location and concentration of radionuclide-labeled radiotracers. Although CT and MRI provide considerable anatomic information about the location and the extent of tumors, these imaging modalities cannot adequately differentiate invasive lesions from edema, radiation necrosis, fibrosis or gliosis (22-24). PET and SPECT have been used to localize and characterize tumors by measuring functional and metabolic activities.

The importance of apoptosis in determining chemotherapy response remains unclear. Some authors have suggested that apoptosis may be the most critical determinant of a tumor's sensitivity or resistance to chemotherapy (25). However, investigations that have studied the importance of apoptosis in human solid tumors have been sparse. Studies of cervical cancer have found the baseline apoptotic index of the malignant cells to be prognostic of clinical response to chemotherapy (26) and overall survival (27). The determination of baseline apoptotic index in breast cancer has been investigated but without definitive indication on the appropriate therapeutic implications of these information (26,27). Therefore, determining the importance of therapy-induced apoptosis in solid tumors currently remains a relatively unexplored area of clinical research. Similarly, the evidence for a spontaneous apoptosis and its relationship with other tumor-related biological features have not been extensively investigated (28).

Extremely limited information is available concerning therapy-induced apoptosis in human tumors because histological evidence of apoptosis occurs within a brief period immediately after treatment. In vivo work has revealed that apoptosis of breast cancer cells rapidly increases to a peak after chemotherapy, and then rapidly declines to baseline levels with an increase in the apoptotic index from 2.5% at baseline to over 20% following treatment (28-30). These studies suggest that apoptosis may be a significant contributor to treatment-induced cell death. In the murine mammary carcinoma, the time of greatest therapy-induced apoptosis was 24-40 hours after initiation of chemotherapy (31). Whether this is the optimal time in human breast cancer patients is currently unknown. The biological differences in humans and mice, as well as differences in the method of chemotherapy delivery, lead us to conclude that sequential biopsies over a period of 2 days is required to determine when therapy-induced apoptosis should be assessed. We investigated whether changes in tumor cell apoptosis and Bcl-2 expression immediately after chemotherapy correlated with response to breast cancer treatment (32). In the previous study, serial core biopsies of 25 breast cancer primary tumors were performed at either two or three time points: before treatment (N = 24) and approximately 24 hours (N = 22) and/or 48 hours (N = 19) after the initiation of the first cycle of chemotherapy. Apoptosis levels were quantified by use of a fluorescent terminal deoxynucleotidyl transferase-mediated deoxyuridine triphosphate nick end-labeling (TUNEL) stain, and Bcl-2 and Bax were measured by semiquantitative immunohistochemical assays. The apoptosis level at 48 hours was significantly higher in the tumors with pathological complete response or < 1 cm of residual disease (median, 22%; range, 6%-51%) than in the tumors with > 1 cm residual disease (median, 7%; range, 1%-36%); P = 0.05 (Mann-Whitney test). A decrease in Bcl-2 expression after chemotherapy relative to the expression from the pretreatment sample also correlated with disease response. Specifically, three of the nine tumors with a decrease in Bcl-2 had a pathological complete response, compared with 0 of the 15 tumors with stable levels of Bcl-2 (Fisher's exact test). There was no relationship between serial measurements of Bax and response. These data suggested that apoptosis may play an important role in determining breast cancer response to chemotherapy and that the level of treatment-induced apoptosis may have some value as a predictive marker.

This clinical study demonstrated that ^{99m}Tc EC-annexin V can localize and image primary invasive breast cancer with a median signal ratio that it is double compared to normal tissue (internal control). The morphological description of the primary lesion and local lymph nodes provide functional baseline information on the disease. This is the first indication that using an imaging modality we can evaluate and describe the presence of spontaneous apoptosis. Additionally, this technology has potential to detect treatment-related apoptosis. The importance of the baseline apoptotic index in breast cancer has never been investigated, and determining the importance of therapy-induced apoptosis in solid tumors currently remains a relatively unexplored area of clinical research. In fact, in the 9 patients, the ^{99m}Tc EC-annexin V accumulated well in breast cancer lesions. In the images of figure 3, there are some

discrepancies between visual lesion intensity and T/N ratio. These discrepancies were shown in the cases of before treatment, and might be based on the relatively high SPECT value of ROI in control area in patients before treatment. However, the mechanisms of ^{99m}Tc EC-annexin V uptake into non-tumor cell before and after treatment still remain unclear. Higher values of T/N are associated with complete or partial remission. The mean T/N baseline with and without the chemotherapy administration was 2.6 and 1.5, respectively (figure 5). Therefore, these early data suggest that ^{99m}Tc EC-annexin V may be an expected candidate of SPECT ligand to evaluate the baseline level of apoptosis, predict the efficacy of therapy based on the detection of treatment-related apoptosis and possibly predict disease progression and prognosis. Furthermore, it appears to correlate with biological markers of proliferation, suggesting a correlation with the occurrence of spontaneous apoptosis.

From the clinical-image based dosimetric study, the total EDEs for single injection dosage of 925-1073 MBq of ^{99m}Tc EC-annexin V were calculated to be 6.80-7.89 mSv. These numbers were less than the annual occupational dose limits of 50 mSv and the annual effective dose limit to individual workers of 30 mSv, which are recommended by International Commission on Radiological Protection (ICRP 60) and Atomic Energy Regulatory Board (AERB), respectively. The highest radiation dose equivalent to an organ for the proposed single injection dosage were 8.65-10.03 mSv, shown in the liver, and these numbers were less than 150 mSv, the limit of annual dose equivalent to a sensitive organ, lens of eye (ICRP 60). As for the clinically approved radiopharmaceuticals, for example, the total EDEs for 740MBq injection of ^{99m}Tc-MDP and 111MBq injection of ^{67}Ga-citrate has been evaluated to be 2.0 mSv and 7.8 mSv, respectively (33). The total EDE for ^{99m}Tc EC-annexin V of 6.80-7.89 mSv could be reasonable and allow it for clinical use.

In summary, a simple labeling method for preparation of high specific activity ^{99m}Tc EC-annexin V was developed. Our clinical findings indicate that ^{99m}Tc EC-annexin V may be an expected candidate of SPECT ligand as a biomarker imaging for evaluating the treatment related apoptosis after induction chemotherapy.

Acknowledgements

The authors wish to thank Charhonda Chilton for her secretarial support. This work was supported in part by the John S. Dunn Foundation and Cell>Point Biotechnology Company (LS01-212). The animal research was supported by M. D. Anderson Cancer Center (CORE) Grant NIH CA-16672.

References

1. Buchholz TA, Hunt KK, Whitman GJ, et al. Neoadjuvant chemotherapy for breast carcinoma: multidisciplinary considerations of benefits and risks. Cancer 2003;98(6):1150–60. [PubMed: 12973838]
2. Cole BF, Gelber RD, Gelber S, et al. Polychemotherapy for early breast cancer: an overview of the randomised clinical trials with quality-adjusted survival analysis. The Lancet 2001;358(9278):277–86.
3. Fisher B, Bryant J, Wolmark N, et al. Effect of preoperative chemotherapy on the outcome of women with operable breast cancer. J Clin Oncol 1998;16(8):2672–2685. [PubMed: 9704717]
4. Bear HD, Anderson S, Brown A, et al. The effect on tumor response of adding sequential preoperative docetaxel to preoperative doxorubicin and cyclophosphamide: preliminary results from National Surgical Adjuvant Breast and Bowel Project Protocol B-27. J Clin Oncol 2003;21(22):4165–74. [PubMed: 14559892]
5. Green MC, Buzdar AU, Smith T, et al. Weekly Paclitaxel Improves Pathologic Complete Remission in Operable Breast Cancer When Compared With Paclitaxel Once Every 3 Weeks. Journal of Clinical Oncology 2005;23(25):5983–5992. [PubMed: 16087943]

6. Pusztai L, Ayers M, Stec J, et al. Gene expression profiles obtained from fine-needle aspirations of breast cancer reliably identify routine prognostic markers and reveal large-scale molecular differences between estrogen-negative and estrogen-positive tumors. Clin Cancer Res 2003;9(7):2406–15. [PubMed: 12855612]
7. Brock CS, Meikle SR, Price P. Does ^{18}F-fluorodeoxyglucose metabolic imaging of tumors benefit oncology? Eur J Nucl Med 1997;24(6):691–705. [PubMed: 9169580]
8. Goldsmith SJ. Receptor imaging: Competitive or complementary to antibody imaging. Semin Nucl Med 1997;27(2):85–93. [PubMed: 9144853]
9. Ogura Y, Krams SM, Martinez OM, et al. Radiolabeled annexin V imaging: diagnosis of allograft rejection in an experimental rodent model of liver transplantation. Radiology 2000;214(3):795–800. [PubMed: 10715048]
10. Ohtsuki K, Akashi K, Aoka Y, et al. Technetium-99m HYNIC-annexin V: a potential radiopharmaceutical for the in-vivo detection of apoptosis. Eur J Nucl Med 1999;26(10):1251–8. [PubMed: 10541822]
11. Blankenberg FG, Robbins RC, Stoot JH, et al. Radionuclide imaging of acute lung transplant rejection with annexin V. Chest 2000;117(3):834–40. [PubMed: 10713014]
12. Verbruggen A, Nosco D, Van Nerom C, et al. Technetium-99m-L,L-ethylenedicysteine: a renal imaging agent. I. Labeling and evaluation in animals. J Nucl Med 1992;33(4):551–7. [PubMed: 1532419]
13. Canet EP, Casali C, Desenfant A, et al. Kinetic characterization of CMD-A2-Gd-DOTA as an intravascular contrast agent for myocardial perfusion measurement with MRI. Magn Reson Med 2000;43(3):403–9. [PubMed: 10725883]
14. Laissy JP, Faraggi M, Lebtahi R, et al. Functional evaluation of normal and ischemic kidney by means of gadolinium-DOTA enhanced TurboFLASH MR imaging: a preliminary comparison with 99Tc-MAG3 dynamic scintigraphy. Magn Reson Imaging 1994;12(3):413–9. [PubMed: 8007770]
15. Ilgan S, Yang DJ, Higuchi, et al. ^{99m} Tc-Ethylenedicysteine-Folate: A new tumor imaging agent. Synthesis, labeling and evaluation in animals. Cancer Biotherapy and Radiopharm 1998;13(6):427–435.
16. Zareneyrizi F, Yang DJ, Oh C-S, et al. Synthesis of ^{99m}Tc-ethylenedicysteine-colchicine for evaluation of antiangiogenic efffect. Anti-Cancer Drugs 1999;10(7):685–692. [PubMed: 10507319]
17. Yang DJ, Azhdarinia A, Wu P, et al. In Vivo and In Vitro Measurement of Apoptosis in Breast Cancer Cells Using ^{99m}Tc EC-Annexin V. Cancer Biotherapy and Radiopharmaceuticals 2001;16(1):73–84. [PubMed: 11279800]
18. Kumar S, Lennane J, Ratner S. Argininosuccinate synthetase: essential role of cysteine and arginine residues in relation to structure and mechanism of ATP activation. Proc Natl Acad Sci U S A 1985;82 (20):6745–9. [PubMed: 3863125]
19. Stabin M. MIRDOSE: the personal computer software for use in internal dose assessment in nuclear medicine. J Nucl Med 1996;37(3):538–46. [PubMed: 8772664]
20. Mendelson MT, Oestereicher N, Port PL, et al. Breast density as a predictor of mammographic detection: comparison of interval and screen-detected cancers. J Natl Cancer Inst 2000;92(13):1081–1087. [PubMed: 10880551]
21. Ando Y, Fukatsu H, Ishiguchi T, et al. Diagnostic utility of tumor vascularity on magnetic resonance imaging of the breast. Mag Reson Imaging 2000;18(7):807–813.
22. Nowak B, Di Martino E, Janicke S, et al. Diagnostic evaluation of malignant head and neck cancer by F-18-FDG PET compared to CT/MRI. Nuklearmedizin 1999;38(8):312–8. [PubMed: 10615664]
23. Kihlstrom L, Karlsson B. Imaging changes after radiosurgery for vascular malformations, functional targets, and tumors. Neurosurg Clin N Am 1999;10(2):167–80. [PubMed: 10099102]
24. Barker FG, Chang SM, Valk PE, et al. 18-Fluorodeoxyglucose uptake and survival of patients with suspected recurrent malignant glioma. Cancer 1997;79(1):115–26. [PubMed: 8988735]
25. Denmeade SR, Isaacs JT. Programmed cell death (apoptosis) and cancer chemotherapy: Cancer Control. Cancer Control 1996;3(4):303–309. [PubMed: 10765221]
26. Archer CD, Parton M, Smith IE, et al. Early changes in apoptosis and proliferation following primary chemotherapy for breast cancer. British Journal of Cancer 2003;89(6):1035–41. [PubMed: 12966422]

27. Shrinivas P, Abraham E, Ahamed I, et al. Apoptotic index: use in predicting recurrence in breast cancer patients. Journal of Experimental & Clinical Cancer Research 2002;21(2):233–8.

28. Grigoriev MY, Pozharissky KM, Hanson KP, et al. Expression of caspase-3 and -7 does not correlate with the extent of apoptosis in primary breast carcinomas. Cell Cycle 2002;1(5):337–42. [PubMed: 12461296]

29. Wheeler JA, Stephens LC, Tornos C, et al. ASTRO research fellowship: apoptosis as a predictor of tumor response to radiation in stage IB cervical carcinoma. Int J Rad Oncol Biol Phys 1995;32(5): 1487–1493.

30. Meyn RE, Stephens LC, Hunter NR, et al. Induction of apoptosis in murine tumors by cyclophosphamide. Cancer Chem Pharm 1994;33(5):410–414.

31. Meyn RE, Stephens LC, Hunter NR, et al. Kinetics of cisplatin-induced apoptosis in murine mammary and ovarian adenocarcinomas. Int J Cancer 1995;60(5):725–729. [PubMed: 7860148]

32. Meyn RE, Stephens LC, Hunter NR, et al. Apoptosis in murine tumors treated with chemotherapy agents. Anti-Cancer Drugs 1995;6(3):443–450. [PubMed: 7670143]

33. Hisada, K.; Tonami, N.; Kubo, A., et al. A new textbook of clinical nuclear medicine. 3. Kanehara & Co LTD; Tokyo: 1999. p. 696-697.

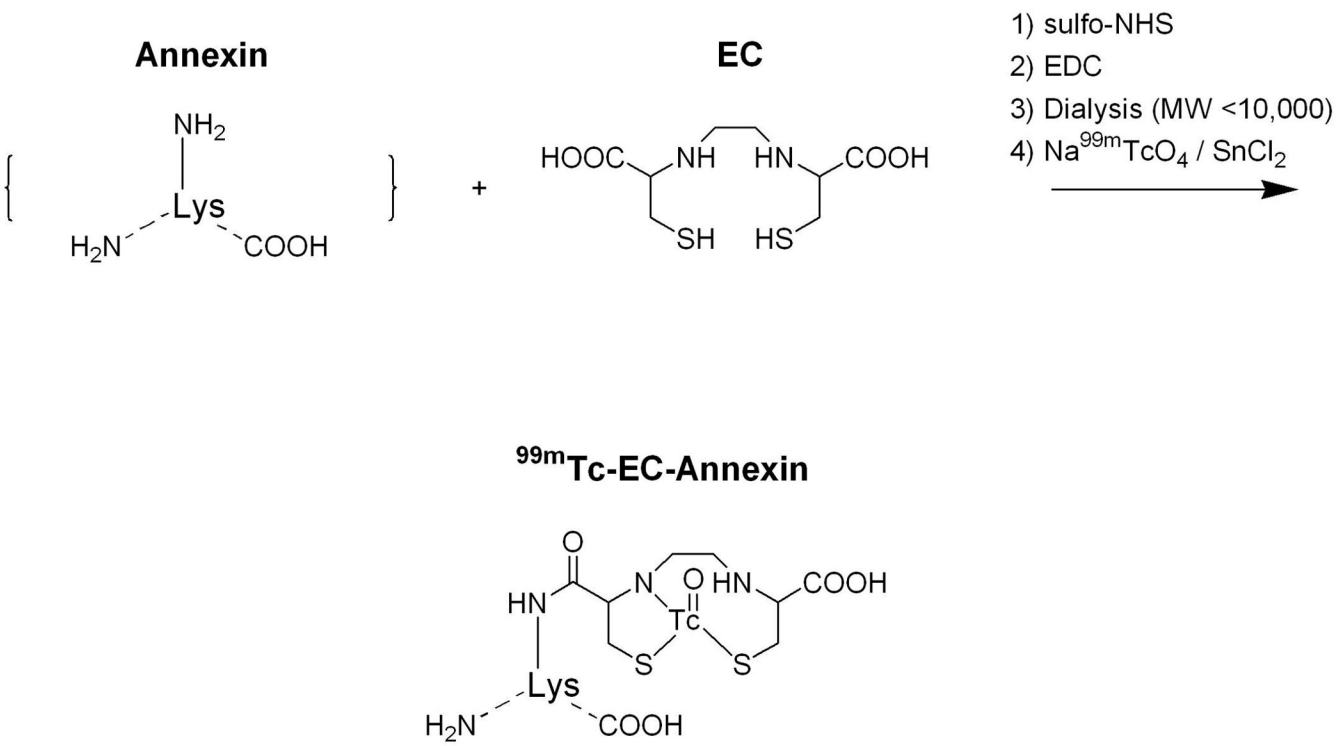

FIGURE 1.
Synthesis of ^{99m}Tc EC-Annexin V

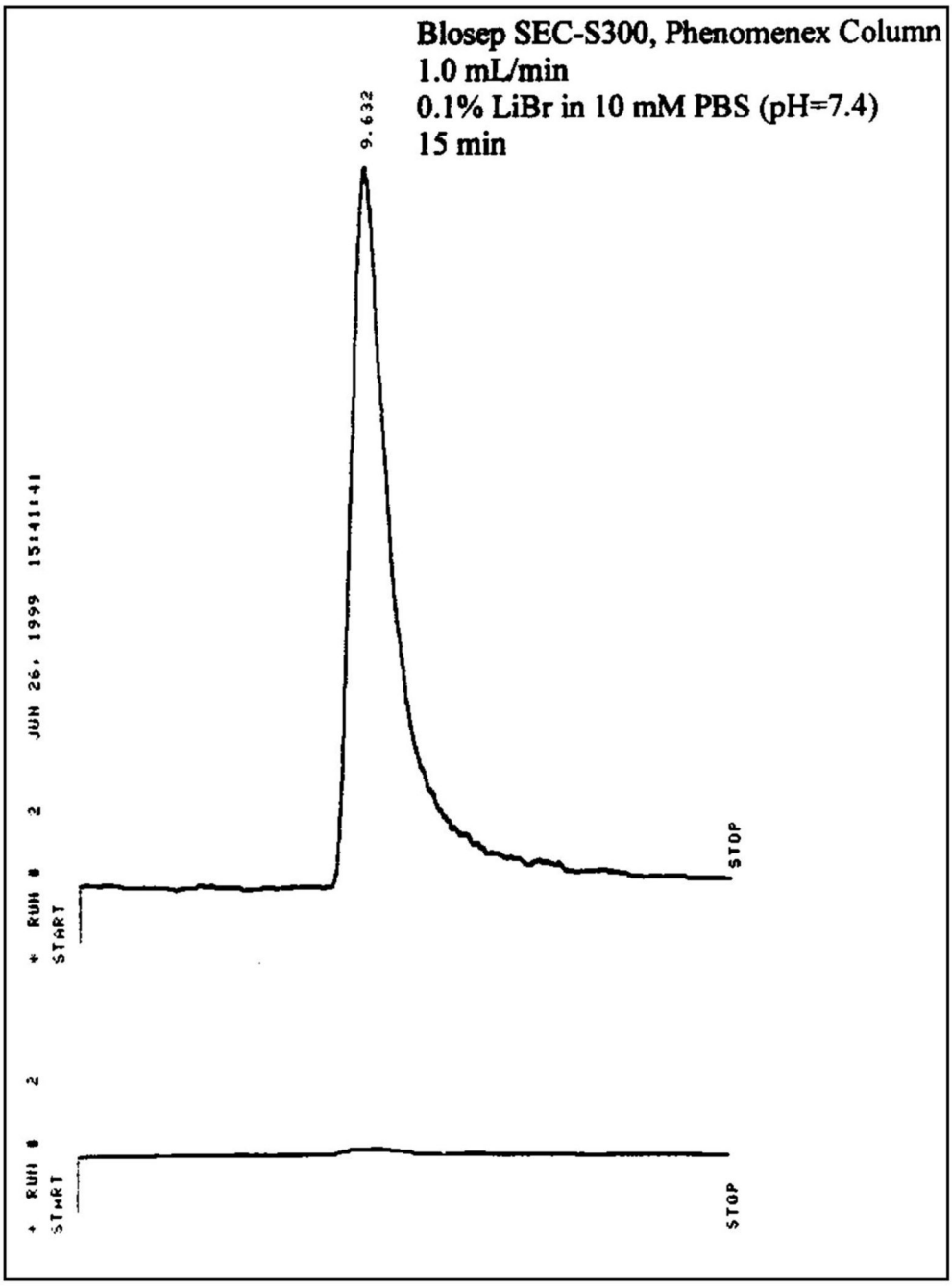

FIGURE 2.

High performance liquid chromatographic (HPLC) analysis of ^{99m}Tc EC-Annexin V (top: radioactive detector, bottom: UV detector at 254 nm) showed that radiochemical purity was >99%.

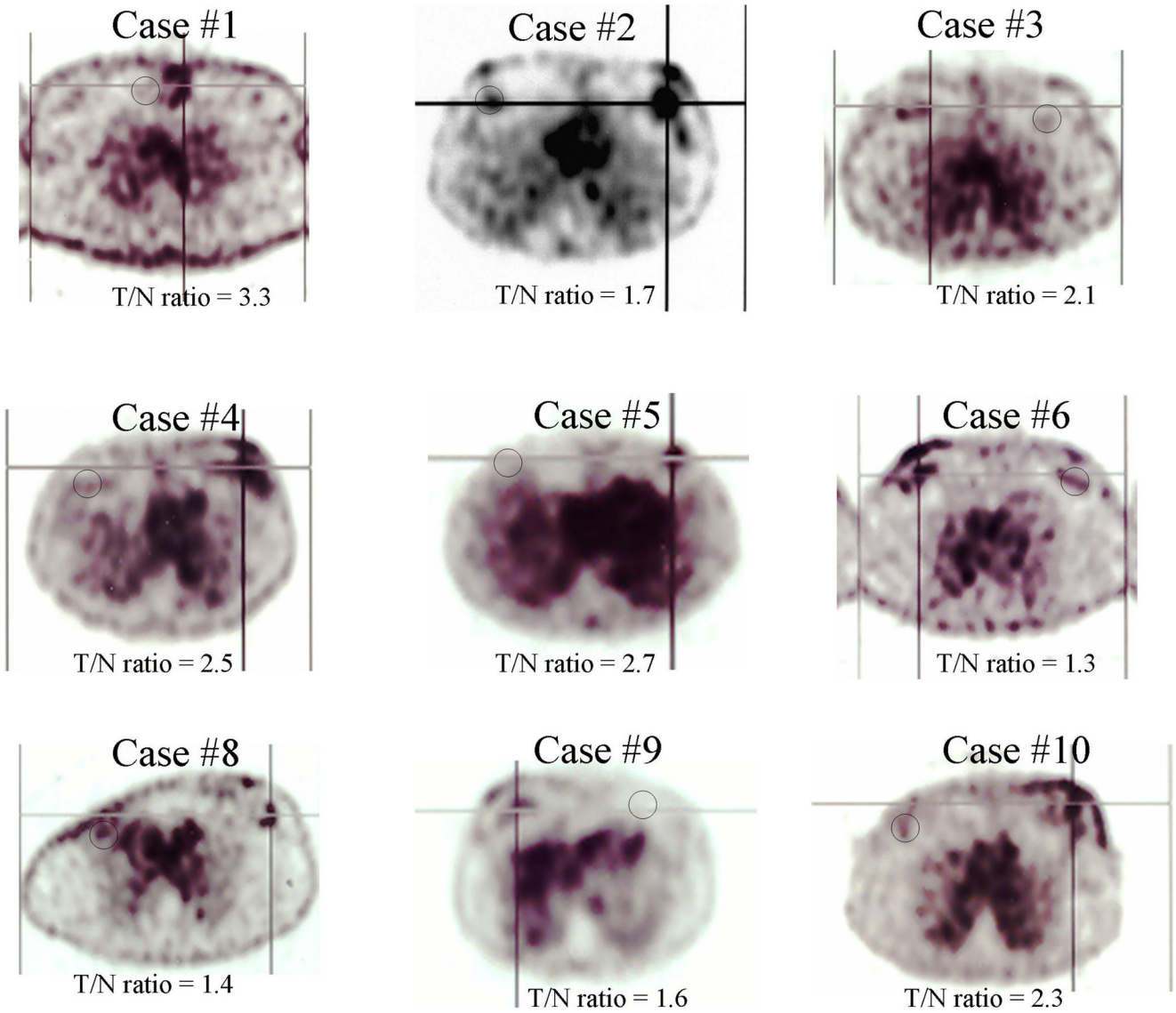

FIGURE 3.

Axial images of patients who received ^{99m}Tc EC-annexin V (925-1073MBq, iv, 3 hours) showed that the tumors could be well visualized. Cross-line indicates ROI of tumor, and black circle indicates ROI of control. One patient showed high uptake in the lung, indicating colloid formation (case #7, image not shown).

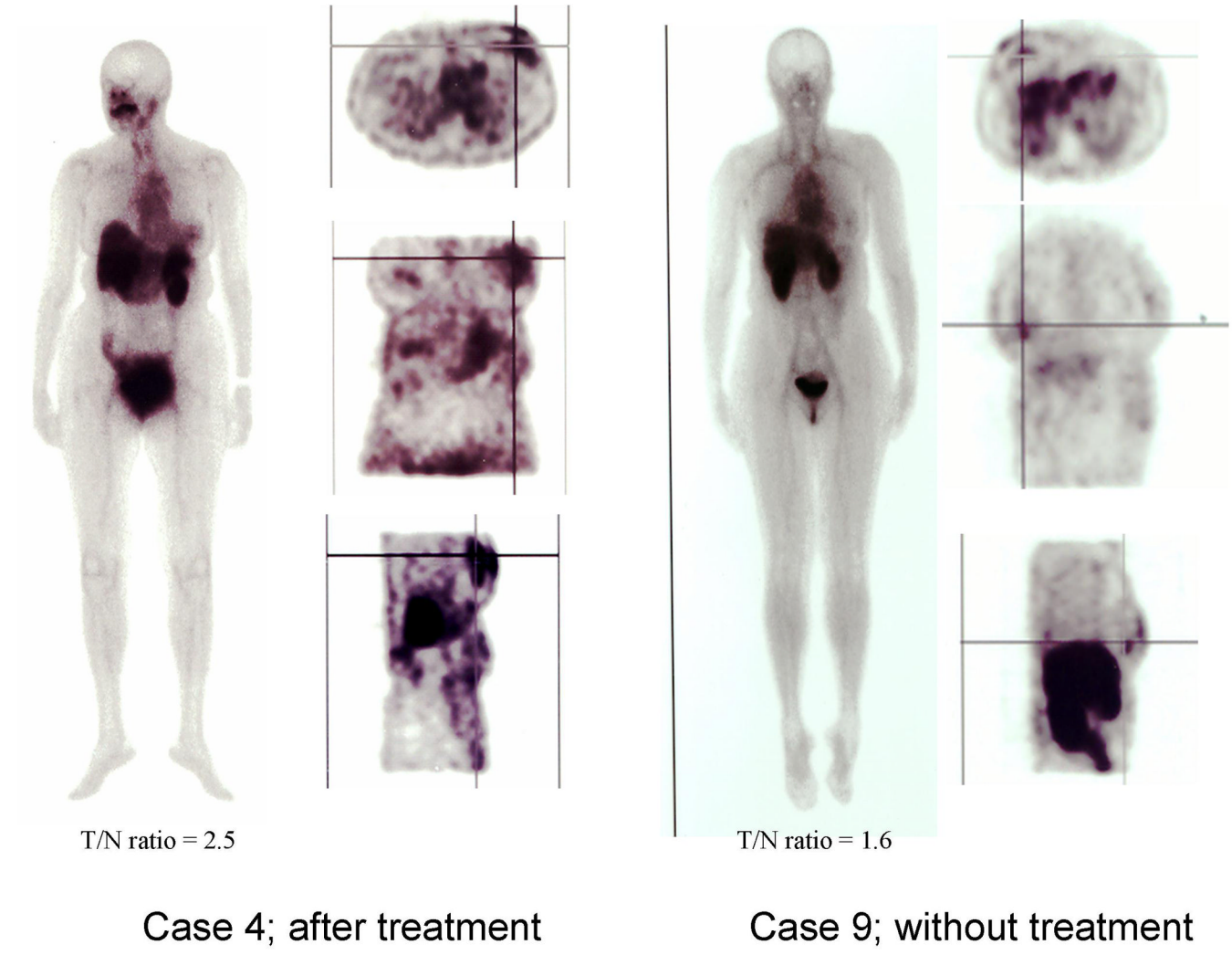

FIGURE 4.
Typical images of patients after treatment and without treatment. Crossed line indicates tumor location. The higher T/N ratio was obtained in the case of after treatment (case 4) as compared to the untreated case (case 9).

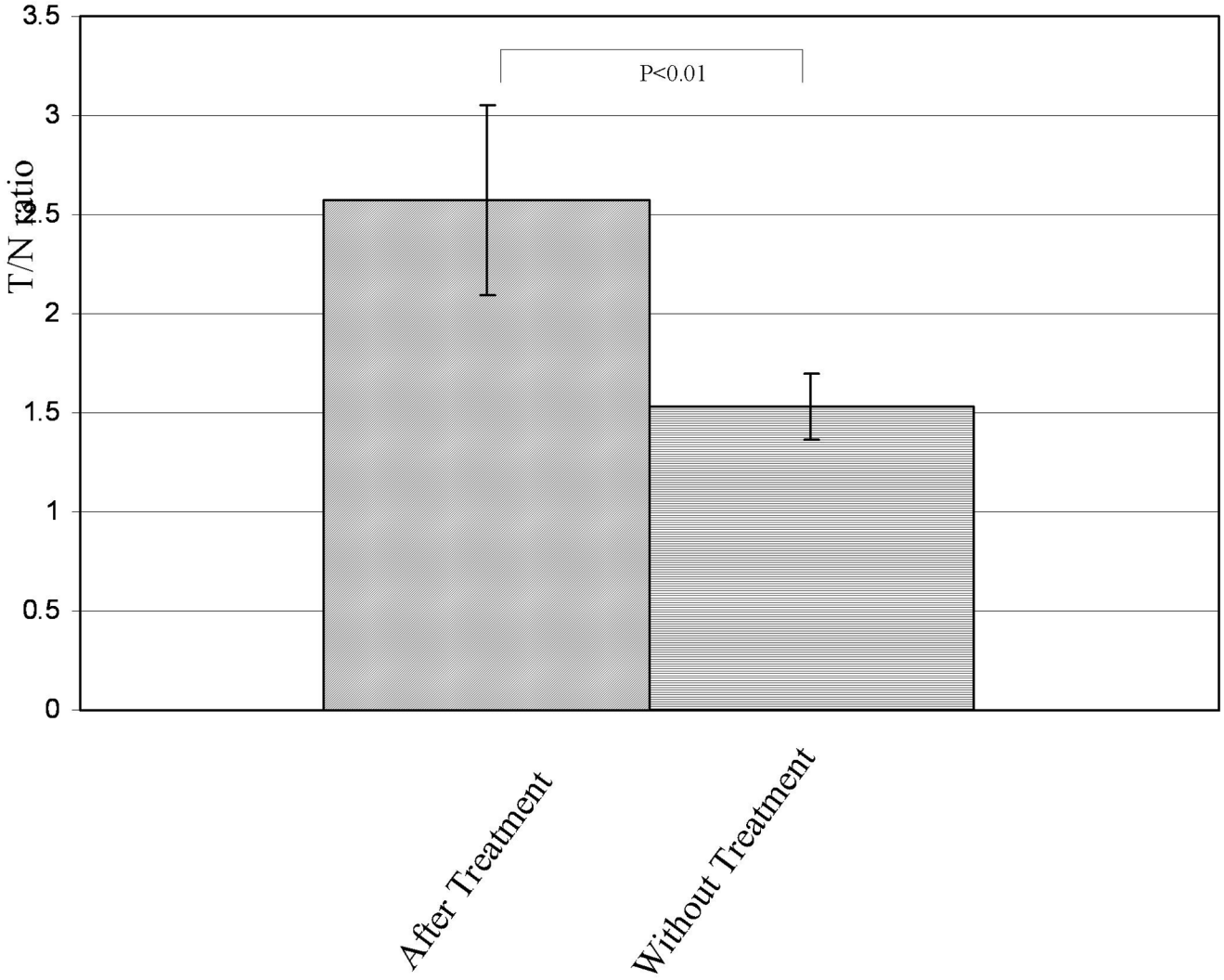

FIGURE 5.
Tumor-to-non tumor count density (T/N) ratios with and without treatment. The mean value of T/N ratio with treatment was 2.6±0.5, significantly higher than that of without treatment (1.5±0.2).

Table 1

Summary for the Status of Breast Tumor Patients

Case	Tumor Size (cm)	Stage	Pathology	Black's Nuclear Grade	ER and/or PR	Her-2/neu	Ki-67 (%)	Treatment before Imaging	Response to Initial treatment	T/N ratio
1	3.5 × 4	II	poorly differentiated invasive ductal carcinoma	3	negative	negative	N/A	Genasense	PR	3.3
2	5 × 5	III	poorly differentiated invasive ductal carcinoma	3	negative	negative	30	-	-	1.7
3	3 × 5	II	Invasive ductal carcinoma	2	positive	negative	10	Paclitaxel	CR	2.1
4	6 × 5	III	Invasive adeno carcinoma	2	positive	negative	75	FAC	PR	2.5
5	3.5 × 4	II	poorly differentiated invasive ductal carcinoma	3	positive	negative	40	Paclitaxel	CR	2.7
6	8 × 6	III	moderately differentiated infilterating ductal carcinoma	2	positive	negative	N/A	-	-	1.3
7*	3.5 × 4	II	poorly differentiated tumor	3	positive	negative	N/A	-	-	N/A
8	5 × 4	III	moderately differentiated infilterating ductal carcinoma	2	positive	negative	90	-	-	1.4
9	3 × 4	II	poorly differentiated infilterating lobular carcinoma	3	positive	positive	35	-	-	1.6
10	5 × 5	III	poorly differentiated invasive ductal carcinoma	3	positive	positive	20	Genasense	PR	2.3

CR: complete remission, PR: partial remission

* The data was not available due to colloidal formation in final product

TABLE 2

Radiation Dose Estimates from human (n=9) for the REFERENCE ADULT using ^{99m}Tc EC-ANNEXIN V

TARGET ORGAN	Average Gy/MBq
Adrenals	**5.83E-06**
Brain	**2.78E-06**
Breasts	**2.69E-06**
Gallbladder Wall	**5.97E-06**
LLI Wall	**4.81E-06**
Small Intestine	**4.54E-06**
Stomach	**4.49E-06**
ULI Wall	**4.76E-06**
Heart Wall	**4.65E-06**
Kidneys	**2.00E-05**
Liver	**9.35E-06**
Lungs	**7.59E-06**
Muscle	**3.46E-06**
Ovaries	**4.92E-06**
Pancreas	**5.76E-06**
Red Marrow	**3.70E-06**
Bone Surfaces	**6.24E-06**
Skin	**2.22E-06**
Spleen	**9.27E-06**
Thymus	**3.70E-06**
Thyroid	**3.57E-06**
Urin Bladder Wall	**2.25E-05**
Uterus	**5.70E-06**
Total Body	**3.92E-06**
Effective dose equivalent (mSv/MBq)	**7.35E-03**
Effective dose (mSv/MBq)	**6.30E-03**